2015 International Symposium on Nonlinear Theory and its Applications
NOLTA2015, Kowloon, Hong Kong, China, December 1-4, 2015

Generation of broadband chaotic signals in subterahertz range basing on semiconductor superlattice for communication systems with chaotic carriers

A.E. Hramov†, A.A. Koronovskii†, S.A. Kurkin†, M. Gaifulin‡, V. Makarov†, V. Maximenko†, N.V. Alexeeva‡, K.N. Alekseev‡, M.T. Greenaway§, T.M. Fromhold§, A. Patanè§, F.V. Kusmartsev‡, O.I. Moskalenko†, and A.G. Balanov‡

†REC 'Nonlinear Dynamics of Complex Systems', Saratov State Technical University
77 Polytechnicheskaja Street, 410056 Saratov, Russia
Faculty of Nonlinear Processes, Saratov State University, 83 Astrakhanskaja Street, 410012 Saratov, Russia
‡Department of Physics, Loughborough University, Loughborough LE11 3TU, United Kingdom
§School of Physics and Astronomy, University of Nottingham, Nottingham NG7 2RD, United Kingdom
Email: hramovae@gmail.com

Abstract—We study both theoretically and experimentally the onset of broadband sub-THz chaos in the miniband semiconductor superlattice. We consider the effects of a external resonator on the high-frequency dynamics of electrons in electronic device exhibiting negative differential conductance. The transition to the broadband chaos, which is confirmed by calculation of Lyapunov exponents, is associated with intermittency scenario. The theoretical findings are confirmed by experimental measurements of a GaAs/AlAs miniband semiconductor superlattice coupled to a microstripe resonator. Our results provide a generic approach for developing modern chaos-based high-frequency technologies including broadband chaotic wireless communication and for super-fast random-number generation.

1. Introduction

Semiconductor superlattices (SLs) are nanostructures formed by several alternating layers of different semiconductor materials [1, 2]. This periodic structure leads to the formation of the energy minibands that enables electrons, in the presence of an electric field, to demonstrate a number of interesting quantum-mechanical phenomena, such as formation of Wannier-Stark ladders, sequential and resonant tunnelling, Bragg reflections, Bloch oscillations, etc. Due to the high mobility of miniband electrons and very high frequency of Bloch and charge-domain oscillations, SLs are considered as the perspective active elements for sub-THz and THz electronic devices [1, 3, 4, 5, 6, 7].

In this report we consider the chaotic subteraherz generation in the SL coupled to a external resonator. The external resonant systems in microwave electronics and telecommunication systems are widely used for tuning and enhancing the characteristics of the high-frequency generation. Besides, coupling of generating device to an external electrodynamic structure sometime leads to emergence of new unexpected phenomena, including bistability [8], self-pulsating [9], and appearance of chaos [10], unfeasible in the isolated devices. Let us note, that possibility to generate sub-THz frequencies (up to 10–200 GHz) chaos in SLs was previously demonstrated both in theory and experiment [11, 12]. These findings have opened wide perspectives for using SL generators in a number of key modern technologies including fast random-number generation [12] and chaos-based communication systems [13, 14]. In the present work we study the dynamical mechanisms responsible for onset of chaos in SL connected to a resonator, and to investigate how the frequency band of chaotic output depend on the voltage applied to the system. In particular, we demonstrate that relative spectral band width of generated chaotic voltage oscillations is very sensitive to applied voltage, and can reach values more than 25% in high-frequency range. The reported results will be useful, e.g. for development and design of high-frequency chaos generators that use SL devices as key elements [12, 15]

2. Model under study and numerical results

We consider a SL interacting with a resonator. We assume that only one EM field mode is excited in the resonator. This mode is characterized by the eigenfrequency, f_Q, and quality factor, Q. In this case the resonator can be represented by the equivalent RLC-circuit and described by the non-stationary Kirchhoff equations (see details in Ref. [10]). The SL serves as a generator of electric current, I, controlled by a voltage, $V_{sl}(t)$, dropped across SL, which includes both the DC supply voltage, V_0, and the AC voltage, $V_1(t)$, generated by the RLC-circuit. To calculate the charge dynamics in the SL, and thus obtain the current-voltage, $I(V_{sl})$, characteristics, we numerically solve the discrete current continuity and Poisson equations. The description of used mathematical model can be found in [10].

The current through the SL is either constant or oscillates depending on the voltage, V_0, applied to the circuit. If the SL is decoupled from the resonator, its current-voltage characteristic, $I(V_{sl})$, is of the Esaki-Tsu type [1] and the oscillations are always periodic. However, if the resonator is coupled to the SL, the behavior changes greatly.

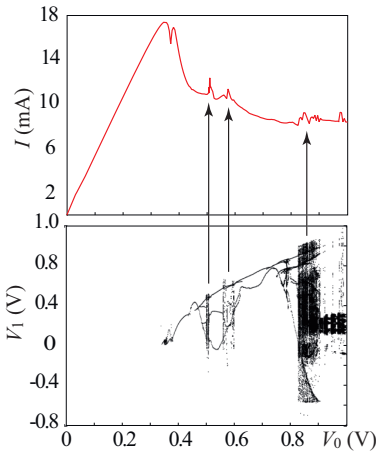

Figure 1: (a) $I(V_0)$ calculated for a SL coupled to a resonator with $f_Q = 13.81$ GHz and $Q = 150$. (b) The bifurcation diagram of $V_1(t)$ vs. V_0

In the coupled regime, the $I(V_{sl})$–characteristic is shown in Fig. 1(a). This dependence has a similar form to the Esaki-Tsu curve. For low voltages, it is ohmic. Thereafter, the current tends to decrease with increasing V_0 due to the onset of Bloch oscillations. However, for $V_0 > V_{crit}$ there is a series of peaks in $I(V_0)$, which do not occur in the absence of the resonator. These peaks correspond to the transitions between different periodic and chaotic dynamical regimes. To illustrate this, in Fig. 1(b) we superimpose a bifurcation diagram in which each point shows the local maximum value of $V_1(t)$ obtained for each V_0 value. Fig. 1 reveals that each peak in the $I(V_0)$ curve corresponds to a transition between different types of dynamics (shown by arrows in Fig. 1) in the bifurcation diagram. With increasing V_0, the dynamics changes first from a steady state solution to periodic oscillations. Thereafter, increasing V_0 induces multiple transitions between periodic and aperiodic oscillations, with each transition corresponding to a peak in the $I(V_0)$ curve. For example, when $V_0 \approx 0.5$ V and $V_0 \approx 0.83$ V, we find peaks in the $I(V_0)$ curve and a transition between periodic and chaotic dynamics.

Note, the SL demonstrates a transition to chaos through intermittency with increase of the DC voltage, V_0. For $V_0 < 510.69$ mV (before the transition to chaos) periodical regime is observed. Increasing the supply voltage ($V_0 > 510.69$ mV) leads to a significant change in the dynamics of the system. The dynamics of the V_1–oscillations features time intervals of the periodic motion (laminar phases) persistently and intermittently interrupted by sudden nonregular phases of oscillations (turbulent phases). If we further increase the supply voltage ($V_0 = 510.75$ mV), fast growth of number of turbulent phases is observed. Described behavior allows us to suppose that transition to chaos goes through intermittency, where the observation voltage difference ($V_0 - V_{0crit}$) being a criticality parameter. For the chosen set of the parameters we estimate

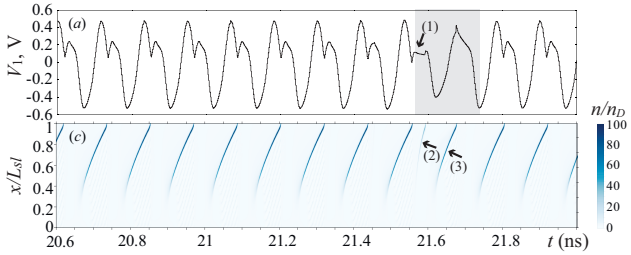

Figure 2: Time series of voltage $V_1(t)$ in resonator (a) and spatio-temporal distributions of charge $n(x,t)$ in SL illustrated domain transport (b) for the bias voltage $V_0 = 510.75$ mV. Turbulent phase is marked by grey

$V_{0crit} = 510.69$ mV. To get deeper insight in intermittent dynamics observed, we investigate how the mean length of laminar phase $\langle\tau\rangle$ changes with increase of voltage V_0 and shown that this dependence is close to the power law with exponent -0.5 $\langle\tau\rangle = \alpha(V_0 - V_{0crit})^{-0.5}$, which confirms the development of type–I intermittency [17].

To understand the physical processes leading to the intermittency chaotic behaviour we analyse time realisation of $V_1(t)$ (Fig. 2 (a)) together with the corresponding spatio-temporal pattern of charge density $\rho(t,x)$ [Fig. 2 (b)] in SL. The $n(t,x)$–value is presented by a color scale in the units of the doping density n_D. Figure 2 reveals that the laminar phases of $V_1(t)$ are characterised by regular behaviour of high-density charge domains travelling along the SL. Each domain is generated, when the values of V_1 achieves minimum. This time moment corresponds to the maximal value of $V_{sl} = V_0 - V_1$, which triggers domain formation, and while a domain propagates along the SL, no new domains can be generated. Note, that the decoupled SL and the resonator have different characteristic time scales. However, for small V_0, the interaction of the resonator and the SL coordinates oscillations of $I(t)$ and the resonator response $V_1(t)$. Growth of V_0 leads to increase of the amplitude of $I(t)$, which excites the resonator. Therefore, the response of resonator $V_1(t)$ becomes more powerful. Occasionally, interaction of the SL and the resonator produces a phase slip between $I(t)$ and $V_1(t)$, which leads to local decrease of V_1 [arrow (1) in Fig. 2(a)], and thus growth of V_{sl}. Eventually, raising V_{sl} exceeds the threshold value, and launches an additional domain [arrow (2) in Fig. 2(b)], which imposes disorder in the queue of domains. This causes further perturbations in $I(t)$ forming a turbulent phase in $V_1(t)$. A slight increase of V_0 makes the phase slips more often, which develops the chaos.

3. Experimental results

To verify our theoretical predictions, we performed experimental measurements on a SL with parameters corresponding to those of our model. The SL was grown by molecular beam epitaxy on a (100)-oriented n-doped

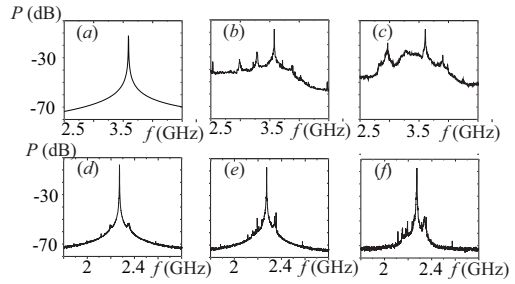

Figure 3: The numerically (*a-c*) and experimentally (*d-f*) obtained power spectra for the SL coupled to two resonators with V_0 = (*a*) 0.42 V, (*b*) 0.43 V, (*c*) 0.44 V; (*d*) 0.34 V, (*e*) 0.35 V, (*f*) 0.355 V.

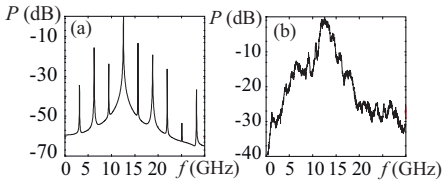

Figure 4: Power spectra for (a) V_0 = 830 mV; and (b) V_0 = 863 mV for f_Q = 13.81 GHz and Q = 150

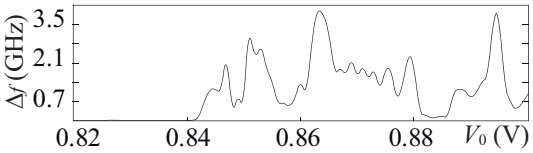

Figure 5: Bandwidth (in GHz) vs. the bias voltage V_0

GaAs substrate. It comprises 15 unit cells, which are separated from two heavily n-doped GaAs contacts by Si-doped GaAs layers of width 50 nm and doping density 1×10^{23} m^{-3}. Each unit cell, of width d and Si doped at 3×10^{22} m^{-3}, is formed by a 1 nm thick AlAs barrier and a 7 nm wide GaAs quantum well with 0.8 InAs monolayers at the center of each QW. The InAs layer facilitates the direct injection of electrons into the lowest energy miniband and also creates a large enough minigap to prevent interminiband tunneling. For electrical measurements, the SL was processed into circular mesa structures of diameter 20 μm with ohmic contacts to the substrate and top cap layer.

The SL was connected to an external high-frequency strip line resonator with a resonant frequency f_{Q2} = 2.38 GHz. Electrodynamic simulations of the SL sample and our direct measurements showed that the contact bonding acts like the parasitic resonator with a resonant frequency of f_{Q1} = 0.87 GHz.

Without the external resonator (when only the parasitic resonator is present), our measurements reveal periodic $V_1(t)$ oscillations with a frequency close to the resonant frequency of the parasitic resonator [16]. However, when the external resonator is connected, the results reveal a transition to chaos, which agrees qualitatively well with our theoretical predictions, see Fig. 3(*d–f*) obtained for the system with two coupled resonators [10]. As V_0 increases, the $V_1(t)$ oscillations and their spectra evolve in a way that reveals the emergence of chaos through the break down of quasiperiodic motion.

The transition from regular oscillations [Fig. 3(*d*)], through quasiperiodic [Fig. 3(*e*)], to chaos [Fig. 3(*f*)] demonstrates experimentally that a linear resonator can induce chaos in a non-linear system. The difference in the frequencies of the experimental and theoretical spectra might be explained by the fact that all experimental measurements were performed at room temperature, but to simplify the model in the numerical simulation T = 4.2 K. The resonator imposes a new oscillatory timescale in the system, thus inducing quasiperiodic current oscillations. Under certain conditions, when the nonlinear mixing of oscillations with different time scales is strong enough, the quasiperiodic motion loses its stability [17], which leads to the appearance of chaos in the system.

4. Broadband sub-THz generation

To gain further insight into chaotic regimes realizing in the SL we consider the wide area of chaotic dynamics, located at high supply voltage $V_0 > 840$ mV. Note, this region of chaos is characterised by more powerful oscillations of $V_1(t)$, and has much less prominent periodic windows, which alternates with chaos with variation of V_0.

The evolution of the spectrum of the Lyapunov exponents corresponding to this transition confirms the presence of chaotic dynamics. We have analyzed the dependencies of four largest Lyapunov exponents Λ_i upon V_0 calculated by method discussed in [18]. For $V_0 < 841$ mV the largest Lyapunov exponent is $\Lambda_1 = 0$, whereas $\Lambda_{2-4} < 0$. Such spectrum of the Lyapunov exponent evidences generation of periodic current and voltage oscillations. With increase of V_0 exponent Λ_1 becomes positive, Λ_2 grows to be zero, and Λ_{3-4} remain negative. Appearance of a positive Lyapunov exponent corresponds to the chaos onset.

In order to study the spectral characteristics of the generated signals, we calculate power spectral density $S(f)$ of the voltage oscillations in the resonator $V_1(t)$. Figures 4 illustrate typical spectra of $S(f)$ for different values of the bias voltage V_0. For V_0 = 830 mV [Fig. 3(a)] the oscillations of V_1 have a discrete spectrum $S(f)$ with the dominant peak at $f \approx 12.72$ GHz corresponding to the basic frequency of oscillations. The peak is surrounded by harmonics and sub-harmonics delimited by frequency interval $\Delta f \approx 3.18$ GHz. For voltages $V_0 \sim 863$ mV [Fig. 4(b)] the spectra become broadband and continuous, confirming generation of developed chaos for larger values of V_0.

We quantitatively characterise the bandwidth Δ_f of the generated signal which is defined as the difference Δ_f =

$f_{b2} - f_{b1}$ between the upper (f_{b2}) and lower (f_{b1}) boundary of the frequency range, within which the power density exceeds the half of the maximum spectral density, which is observed for the frequency f_m. The dependence of $\Delta_f(V_0)$ for $V_0 > 820\,\text{mV}$ is shown in Fig. 5. For V_0 between 0.820 mV and 0.841 mV the bandwidth of V_1 is practically zero reflecting the periodicity of $V_1(t)$ oscillations. However, when V_0 exceeds 0.841 mV the bandwidth of $V_1(t)$ becomes finite, implicating the onset of chaos. The bandwidth of the corresponding oscillations change significantly between $\sim 650\,\text{MHz}$ for $V_0 = 858\,\text{mV}$ and $\sim 3\,\text{GHz}$. This fact proposes that V_0 can be used for effective controlling the bandwidth of signal generated in the SL. Evidently, the wide-band chaotic regimes can be interesting for development of THz chaotic semiconductor sources for communication systems with chaotic carriers or superlattice–based fast random number generators [10, 12, 15].

5. Conclusion

We demonstrated theoretically and experimentally that the SL coupled to a resonator can generate chaotic sub-THz oscillations of current and voltage. Appearance of chaos was confirmed by calculation of spectra and the Laypunov exponents. Remarkably that variation of V_0 can change the relative bandwidth within a significant range 0–28%. This make the SL promising for for development of broadband sources of chaotic microwaves or superlattice–based fast random number generators [10, 12, 15], which could have applications in high-speed chaotic communications.

Acknowledgments

This work has been supported by the Russian Science Foundation (grant 14–12–00222).

References

[1] L. Esaki, R. Tsu, "Superlattices and negative differential conductivity in semiconductors," *IBM J. Research and Develop*. vol.14, pp.61–65, 1970.

[2] R. Tsu, "Superlattices to nanoelectronics", Elsevier, 2005.

[3] T. Hyart, J. Mattas, K. N. Alekseev, "Model of the influence of an external magnetic field on the gain of terahertz radiation from semiconductor superlattices", *Phys. Rev. Lett.* vol.103, p.117401, 2010.

[4] V. V. Makarov, A. E. Hramov, A. A. Koronovskii, et al, "Sub-terahertz amplification in a semiconductor superlattice with moving charge domains", *Appl. Phys. Lett.* vol.106, p.043503, 2015.

[5] F. Klappenberger, A. Ignatov, S. Winnerl, et al, "Broadband semiconductor superlattice detector for THz radiation," *APL*, vol.78, p.1673, 2001.

[6] M. T. Greenaway, A. G. Balanov, D. Fowler, et al, "Using acoustic waves to induce high-frequency current oscillations in superlattices," *Phys. Rev. B*, vol.81, p.235313, 2010.

[7] V. A. Maksimenko, V. V. Makarov, A. A. Koronovskii, et al, "The effect of collector doping on the high-frequency generation in strongly coupled semiconductor superlattice," *Europhis. Lett.* vol.109, p.47007, 2015.

[8] V. B. Taranenko, I. Ganne, R. J. Kuszelewicz, C. O. Weiss, "Patterns and localized structures in bistable semiconductor resonators," *Phys. Rev. A*. vol.61, p.063818, 2000.

[9] J. Petráček, Y. Ekşioğlu, A. Sterkhova, "Simulation of self-pulsing in Kerr-nonlinear coupled ring resonators", *Opt. Commun.* vol.318, p.147, 2014.

[10] A. E. Hramov, A. A. Koronovskii, S. A. Kurkin, et al, "Subterahertz chaos generation by coupling a superlattice to a linear resonator", *Phys.Rev.Lett.* vol.112, p.116603, 2014.

[11] A. G. Balanov, D. Fowler, A. Patanè, et al, *Phys. Rev. E*. vol.77, p.026209, 2008.

[12] W. Li, I. Reidler, Y. Aviad, et al, "Fast physical random-number generation based on room-temperature chaotic oscillations in weakly coupled superlattices", *Phys. Rev. Lett.* vol.111, p.044102, 2013.

[13] A.A. Koronovskii, O.I. Moskalenko, A.E. Hramov, "On the use of chaotic synchronization for secure communication", *Phys.-Uspekhi.* vol.52, p.1213, 2009.

[14] O. I. Moskalenko, A. A. Koronovskii, A. E. Hramov, "Generalized synchronization of chaos for secure communication: Remarkable stability to noise", *Phys. Lett. A*. vol.374, p.2925, 2010.

[15] H. Ren, M. S. Baptista, C. Grebogi, "Wireless communication with chaos", *Phys. Rev. Lett.* vol.110, p.184101, 2013.

[16] N. Alexeeva, M. T. Greenaway, A. G. Balanov, et al, "Controlling high-frequency collective electron dynamics via single-particle complexity", *Phys. Rev. Lett.* vol.109. p.024102, 2012.

[17] H. Schuster, W. Just, "Deterministic chaos," Wiley-VCH, Weinheim, 2005.

[18] A. E. Hramov, A. A. Koronovskii, V. A. Maksimenko, et al, "Lyapunov stability of charge transport in miniband semiconductor superlattices", *Phys. Rev B*. vol.88, p.165304, 2013.